ACS APPLIED MATERIALS & INTERFACES

Research Article

www.acsami.org

Gold Nanoparticle-Based Facile Detection of Human Serum Albumin and Its Application as an INHIBIT Logic Gate

Zhenzhen Huang, Haonan Wang, and Wensheng Yang*

State Key Laboratory of Supramolecular Structure and Materials, College of Chemistry, Jilin University, Changchun 130012, People's Republic of China

Supporting Information

ABSTRACT: In this work, a facile colorimetric method is developed for quantitative detection of human serum albumin (HSA) based on the antiaggregation effect of gold nanoparticles (Au NPs) in the presence of HSA. The citrate-capped Au NPs undergo a color change from red to blue when melamine is added as a cross-linker to induce the aggregation of the NPs. Such an aggregation is efficiently suppressed upon the adsorption of HSA on the particle surface. This method provides the advantages of simplicity and cost-efficiency for quantitative detection of HSA with a detection limit of ~1.4 nM by monitoring the colorimetric changes of the Au NPs with UV−vis spectroscopy. In addition, this approach shows good selectivity for HSA over various amino acids, peptides, and proteins and is qualified for detection of HSA in a biological sample. Such an antiaggregation effect can be further extended to fabricate an INHIBIT logic gate by using HSA and melamine as inputs and the color changes of Au NPs as outputs, which may have application potentials in point-of-care medical diagnosis.

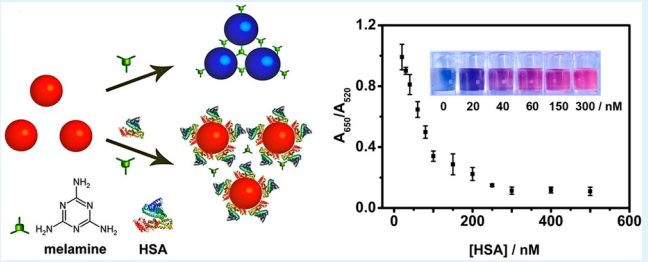

KEYWORDS: *gold nanoparticle, human serum albumin, antiaggregation, detection, logic gate*

INTRODUCTION

Quantitative detection of proteins is of great importance in the field of biochemistry and medicine.[1,2] Human serum albumin (HSA) is the most abundant protein in plasma, which plays vital roles in maintaining the oncotic pressure of blood and serves as a carrier for various substances such as vitamins, fatty acids, drugs, etc. HSA is also important in clinical diagnosis. For example, an elevated concentration of HSA in human urine (>20 mg/L) is a critical indicator for kidney damage, which is associated with diabetes and cardiovascular disease.[3−5] Thus, considerable attention has been focused on quantitative detection of HSA. Immunoassays are one of the most commonly used methods for HSA detection. However, the immunoassays are usually time-consuming and may lead to underestimate of the quantity of albumin.[6,7] High-performance liquid chromatography (HPLC) and liquid chromatography−mass spectrometry (LC−Mass) provide satisfied accuracy and reliability for HSA detection, while the complicated sample pretreatments and expensive instruments limit their application in routine analyses.[8,9] Recently, colorimetric/fluorometric methods have been developed for detection of HSA by employing organic molecular probes with optical activity, which can bind with HSA sepecifically.[10−12] Although the optical methods present acceptable sensitivity and selectivity and are not complicate to operate, syntheses of the organic probes are usually laborious and require the use of toxic solvents. Therefore, it is still highly desirable to develop a more facile and efficient method for HSA detection.

Gold nanoparticles (Au NPs) have been widely used as colorimetric probes for detection of a variety of chemical/biological analytes due to their easy syntheses, good water solubility, and excellent biocompatibility. Especially, Au NPs have a unique optical property termed as surface plasmon resonance (SPR), which is highly dependent on their interparticle distance, that is, the well-dispersed Au NPs exhibit a red color in solution, while the aggregated Au NPs show a blue/purple color.[13−18] Melamine is a well-studied cross-linker for Au NPs. The three primary amine groups of melamine are able to strongly bind on the surface of Au NPs via ligand exchange and result in an extensive aggregation of the Au NPs.[19−21] In this paper, we report that the melamine-induced aggregation of Au NPs can be effectively suppressed upon the adsorption of HSA on the particle surface. On the basis of such an antiaggregation effect, a facile method is developed for detection of HSA by monitoring the colorimetric changes of the Au NPs. This method shows high sensitivity and selectivity and is qualified for quantitative detection of HSA in a biological sample. The antiaggregation effect is extendable to the design and operation of a logic gate. Au NPs have been recognized as ideal candidates for fabrication of colorimetric logic gates, which can transduce specific chemical/biological inputs into optical outputs.[21−24] Here, by using HSA and melamine as inputs and the color changes of Au NPs as outputs, an

Received: September 16, 2014
Accepted: April 8, 2015
Published: April 8, 2015

DOI: 10.1021/acsami.5b01552
ACS Appl. Mater. Interfaces 2015, 7, 8990−8998

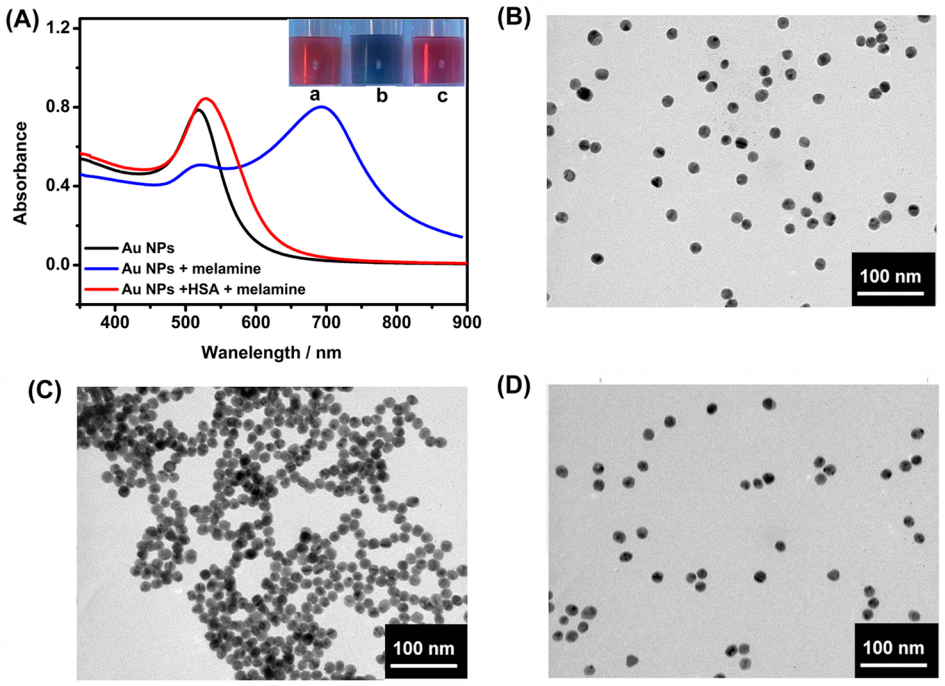

Figure 1. (A) UV−vis spectra and optical photographs (insert) of (a) Au NPs, (b) Au NPs + melamine, (c) Au NPs + HSA + melamine. TEM images of (B) Au NPs, (C) Au NPs + melamine, and (D) Au NPs + HSA+ melamine. Concentrations of the Au NPs, HSA, and melamine used were 2.0 nM, 300 nM, and 20 μM, respectively.

INHIBIT logic gate, which may be potentially useful in point-of-care medical diagnosis, is developed based on the antiaggregation effect.

EXPERIMENTAL SECTION

Materials and Measurements. Hydrogen tetrachloroaurate (III) (≥99.9%), sodium citrate tribasic dehydrate (≥99.0%), and HSA were purchased from Sigma-Aldrich and used without further purification. Melamine and all the amino acids were purchased from Sinopharm Chemical Reagent Co., Ltd. Hemoglobin, horseradish peroxidase (HRP), lysozyme, trypsin, and poly-lysine (M.W. 150, 000−300, 000) were purchased from Sangon (Shanghai, China). Other reagents were all of analytical reagent grade and used as received. UV−vis absorption spectra were acquired by using a Shimadzu UV−1800 spectrophotometer. Transmission electron microscopy (TEM) observations were performed on a JEOL 1200 electron microscope operating at an accelerating voltage of 100 kV using carbon-coated copper grids as substrates. Dynamic light scattering (DLS) measurements were taken on a Brookhaven BI-90 Plus particle size analyzer with a scattering angle of 90°. Circular dichroism (CD) spectra were recorded on a BioLogic scanning spectrometer MOS450 using a rectangular cuvette with a path length of 1 cm. All the experiments unless stated especially were carried out at room temperature (23 ± 2 °C).

Preparation of Au NPs. Citrate-capped Au NPs were prepared according to the modified Frens method.[24,25] In a typical procedure, aqueous solution of $HAuCl_4$ (0.25 mM, 50 mL) was heated under reflux, and then 1.3 mL of sodium citrate (1%) was added under vigorous stirring. The solution was kept on boiling for 15 min. The concentration of the Au NPs (~15 nm) was calculated to be ~2.4 nM by assuming the complete reduction of Au^{3+} to Au^0 atoms.

Determination of the Amount of HSA Adsorbed on Au NPs. The amount of HSA adsorbed on the surface of Au NPs was determined by using the reported methods[26,27] with some modifications. In a typical procedure, a 415 μL dispersion of the Au NPs (2.4 nM) was mixed with 20 μL of HSA with definite concentrations, followed by the addition of 65 μL of pure water. The final volume of all the samples was 500 μL, in which the concentration of Au NPs was 2.0 nM, and those of HSA were 20, 40, 60, 100, and 300 nM, respectively. Three independent samples were prepared for each HSA concentration. The mixtures were incubated at room temperature for 15 min and then centrifuged at 12 000 rpm for 20 min. The supernatants containing the nonadsorbed HSA were transferred to fresh tubes. The amounts of the nonadsorbed HSA in the supernatants were quantified by using Micro BCA Protein Assay Kit (Thermo Scientific, USA). The amounts of HSA adsorbed to the surface of Au NPs were derived by subtracting the amount of nonadsorbed HSA from the total amount of the HSA added initially. The numbers of HSA molecules absorbed on the surface of one Au NP (N) were calculated by using the following equation:

$$N = (C_0 - C_{non})/C_{AuNPs}$$

in which C_0, C_{non}, and C_{AuNPs} represent the molar concentration of HSA added initially, nonabsorbed HSA remained in the supernatants, and Au NPs, respectively.

HSA Assay. In a typical test, a 415 μL dispersion of the Au NPs (2.4 nM) was mixed with 20 μL of HSA with definite concentrations, followed by the addition of 55 μL of pure water. The mixtures were then incubated at room temperature for 15 min before the addition of melamine (10 μL, 1.0 mM). The final volume of the samples was 500 μL, in which the concentrations of the Au NPs and melamine were 2.0 nM and 20 μM, and those of HSA were 20, 40, 60, 80, 100, 150, and 300 nM, respectively. UV−vis absorption spectra were recorded after the addition of melamine for 15 min.

Preparation of Artificial Urine Sample. Artificial urine was prepared according to a standard method shown in previous reports.[28,29] The solution contained lactic acid (1.1 mM), citric acid (2.0 mM), sodium bicarbonate (25.0 mM), urea (170.0 mM), calcium chloride (2.5 mM), sodium chloride (90.0 mM), magnesium sulfate (2.0 mM), sodium sulfate (10.0 mM), potassium dihydrogen phosphate (7.0 mM), dipotassium hydrogen phosphate (7.0 mM), and ammonium chloride (25.0 mM). The pH of the solution was adjusted to 6.0 by addition of hydrochloric acid (1.0 M).

INHIBIT Logic Gate. An aqueous dispersion of the citrate-capped Au NPs (500 μL, 2.0 nM) was added into a tube. The INHIBIT operation was triggered by the addition of the four possible combinations of inputs: (1) H_2O (0, 0); (2) 20 μM melamine (1,

DOI: 10.1021/acsami.5b01552
ACS Appl. Mater. Interfaces 2015, 7, 8990−8998

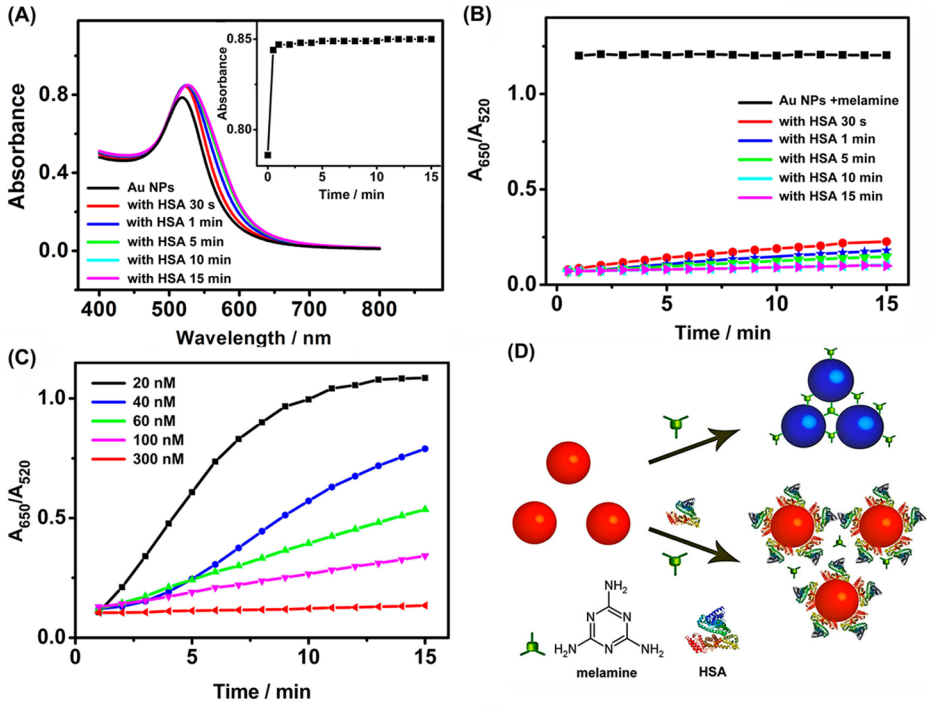

Figure 2. (A) UV−vis spectra of the Au NPs before and after incubation with 300 nM of HSA for different times. Inset: variation in absorbance intensity of the SPR peak of the Au NPs with the incubation time. (B) Variation in A_{650}/A_{520} value of the Au NPs with time after the addition of melamine for the Au NPs incubated with HSA (300 nM) for different times. (C) Variation in A_{650}/A_{520} value of the Au NPs with time after the addition of melamine for the Au NPs incubated with different concentrations of HSA for 15 min. Concentrations of the Au NPs and melamine used were 2.0 nM and 20 μM, respectively. (D) Schematic illustration of the antiaggregation effect.

0); (3) 300 nM HSA (0, 1); (4) 300 nM HSA and 20 μM melamine (1, 1).

RESULTS AND DISCUSSION

Antiaggregation Effect of Au NPs via HSA Adsorption.

As shown in Figure 1, panel A, the citrate-capped Au NPs (2.0 nM) were red in color with a characteristic SPR peak located at 518 nm in UV−vis spectra. Upon the addition of melamine (20 μM), intensity of the absorbance at 518 nm decreased dramatically, while a new broad peak emerged around 690 nm, accompanied by a color change from red to blue due to aggregation of the Au NPs.[19−21] When dispersion of the Au NPs was incubated with HSA (300 nM) for 15 min before the addition of melamine, the SPR peak only shifted from 518 to 529 nm, and there was almost no change in color of the solution, which indicates the suppressed aggregation of the Au NPs. TEM observations further revealed that the well-dispersed Au NPs underwent an extensive aggregation upon the addition of melamine, which was inhibited effectively in the presence of HSA (Figure 1B−D).

It has been known that the adsorption of proteins can induce the change in refractive index of the surrounding medium of the Au NPs and result in the change in both absorbance intensity and position of the SPR peak.[26,30−32] Thus, UV−vis spectra of the Au NPs were recorded to evaluate the absorption process of HSA on the particle surface. As shown in Figure 2, panel A, intensity of the absorbance of the Au NPs (2.0 nM) increased obviously after incubation of the Au NPs with HSA (300 nM) for 30 s, accompanied by a red shift of the SPR peak from 518−526 nm. In the period of 30 s−15 min, there was only little change in absorbance intensity of the SPR peak (inset of Figure 2A), which suggests that the adsorption of HSA on the particle surface is a fast process, which is in consistent with the result reported in previous work.[26] It is supposed that the adsorption of HSA may shield the surface of Au NPs, thus stabilizing the Au NPs and suppressing their aggregation induced by the melamine cross-linker.

To further understand the possible mechanism for the antiaggregation effect, influence of the incubation time on the stability of the Au NPs was investigated by monitoring the changes in absorbance ratio at 650 and 520 nm (A_{650}/A_{520}). The A_{650}/A_{520} is documented to be related to the aggregated and dispersed Au NPs and thus the degree of aggregation of Au NPs.[21,24] As shown in Figure 2, panel B, in the absence of HSA, the value of A_{650}/A_{520} immediately increased to 1.4 by the addition of melamine, which indicates the rapidly extensive aggregation of the Au NPs induced by melamine. Increase of the value of A_{650}/A_{520} became much slower when the Au NPs were incubated with HSA for 30 s or longer. For the Au NPs incubated with HSA for 15 min, addition of melamine resulted in little change of the A_{650}/A_{520} value, which indicates that aggregation of the Au NPs was suppressed greatly upon the absorption of HSA on the particle surface.

The role of HSA in the suppressed aggregation process was further proved by changing its concentration in the incubation. As shown in Figure 2, panel C, the degree of aggregation of the Au NPs was dependent on the concentration of HSA used in the incubation. When the concentration of HSA was 20 nM, the value of A_{650}/A_{520} increased from ∼0.1 to ∼1.1 after the addition of melamine for 15 min. The increase in the A_{650}/A_{520} value became slower with the increased concentration of HSA used. For example, the value only increased from ∼0.1 to ∼0.3 when the concentration of HSA was 100 nM, and almost no increase in the A_{650}/A_{520} value was observed when the

DOI: 10.1021/acsami.5b01552
ACS Appl. Mater. Interfaces 2015, 7, 8990−8998

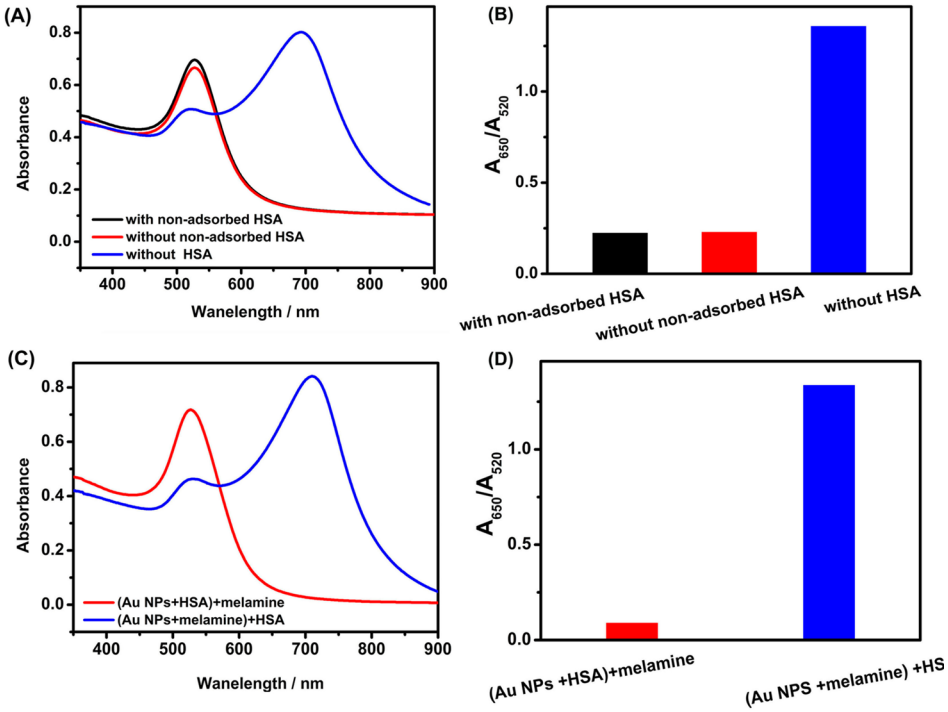

Figure 3. (A) UV−vis spectra and (B) corresponding values of A_{650}/A_{520} of the Au NPs with nonadsorbed HSA, without nonadsorbed HSA, and without HSA by the addition of melamine. (C) UV−vis spectra and (D) corresponding values of A_{650}/A_{520} of the Au NPs with the addition sequences of HSA + melamine and melamine + HSA. Concentrations of the Au NPs, HSA, and melamine used were 2.0 nM, 300 nM, and 20 μM respectively.

concentration of HSA increased to 300 nM. It is expected that more HSA molecules are absorbed on the particle surface under higher concentration of HSA, thus suppressing aggregation of the Au NPs induced by the melamine linker much effectively. Such an antiaggregation effect of HSA can be schematically represented as shown in Figure 2, panel D. When there are enough HSA molecules adsorbed on the particle surface, the melamine-induced aggregation of the Au NPs is suppressed effectively since the protein molecules can provide steric hindrance to stabilize the Au NPs or inhibit the interaction of melamine with the particle surface.

The amounts of HSA adsorbed on surface of the Au NPs were investigated to illustrate the assumption that more protein molecules were absorbed on the particle surface under higher concentration of HSA. It has been reported that HSA can adsorb on the particle surface as a monolayer either in a "flat-on" or an "end-on" fashion, resulting in an increment of ∼6.4 nm or ∼14.5 nm in size of the particles.[26,30,31] DLS measurements (Supporting Information, Figure S1) showed that hydrodynamic diameter of the Au NPs increased from 20.7 ± 0.1 to 28.4 ± 0.1 nm in the presence of 300 nM HSA. Such an increment in the hydrodynamic diameter (∼7 nm) suggested that a monolayer of the HSA molecules was absorbed on the particle surface mainly in the "flat-on" fashion. By using the Micro BCA Protein Assay Kit and the equation described in the Experimental Section, numbers of the HSA molecules adsorbed on surface of each Au NP were determined to be 3 ± 2, 5 ± 1, 8 ± 3, 17 ± 2, and 21 ± 2, respectively, when the concentrations of HSA used in the incubations were 20, 40, 60, 100, and 300 nM. The theoretical surface area per HSA molecule adsorbed on the Au NPs in the "flat-on" fashion is about 30.6 nm^2, while the total surface area of each 15 nm Au NP is about 706.5 nm^2.[30] Thus, it was deducible that surface coverage of HSA on the Au NPs increased from ∼13% to ∼91% when the concentration of HSA used increased from 20 to 300 nM. These results prove the assumption that more HSA molecules are absorbed on the particle surface under higher HSA concentration. At high concentration of HSA (300 nM), most of the surface of the Au NPs (∼91%) has been covered by the protein molecules. Such a high coverage of HSA is effective to prevent the close approaching of neighboring Au NPs by steric hindrance or inhibit the effective cross-linking of neighboring Au NPs by melamine.

Control experiments were performed to exclude the impact of the nonadsorbed HSA on the antiaggregation effect. The mixture of the Au NPs (2.0 nM) incubated with HSA (300 nM) for 15 min was centrifuged (12 000 rpm, 20 min) to remove the HSA molecules that were not absorbed on the particle surface. The supernatant containing the nonadsorbed HSA was discarded, and precipitation of the Au NPs absorbed with HSA was redispersed in water. As shown in Figure 3, panels A and B, both the samples with and without nonadsorbed HSA exhibited great stability in the presence of melamine (20 μM), which indicates that the nonadsorbed HSA molecules have little contribution to the antiaggregation effect. Influence of the addition sequence of HSA and melamine on the antiaggregation effect was also investigated. As illustrated in Figure 3, panels C and D, when HSA was added into dispersion of the Au NPs first, aggregation of the Au NPs was suppressed effectively. However, when melamine was added into the dispersion first, subsequent addition of HSA had little impact on suppressing the aggregation of the Au NPs. It is known that melamine can weakly bind to the protein molecule through hydrogen bond interactions.[33] It is likely that such weak interactions are not effective for HSA to replace the melamine from the particle surface. These results further support the

DOI: 10.1021/acsami.5b01552
ACS Appl. Mater. Interfaces 2015, 7, 8990−8998

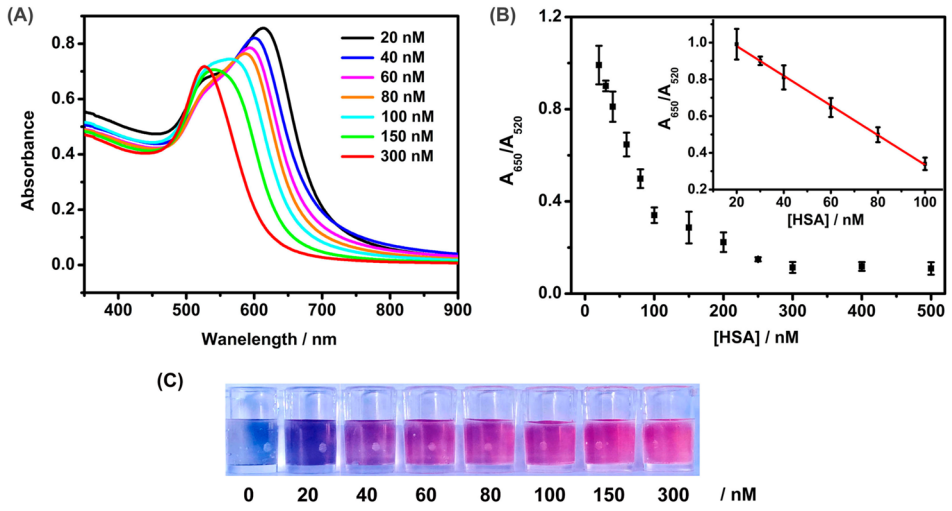

Figure 4. (A) UV−vis spectra, (B) variations in values of A_{650}/A_{520}, and (C) optical photographs of the Au NPs incubated with different concentrations of HSA for 15 min, followed by the addition of melamine. Insert of panel B gives a linear plot of A_{650}/A_{520} vs HSA concentration ($y = -0.0081x + 1.1$, $R^2 = 0.99$). Concentrations of the Au NPs and melamine used were 2.0 nM and 20 μM, respectively.

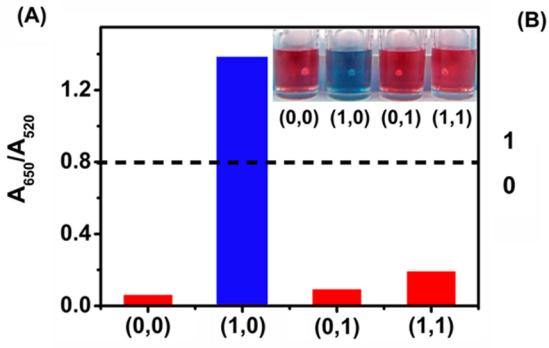

(B)

Input		Output
melamine	HSA	
0	0	0
1	0	1
0	1	0
1	1	0

Figure 5. (A) Values of A_{620}/A_{520} and (B) truth table of the INHIBIT gate in the presence of different inputs. Inset of pane A gives optical photographs of the corresponding samples.

conclusion that the antiaggregation effect is contributed by HSA adsorbed on the particle surface rather than the interactions between HSA and melamine.

Other aggregating agents of Au NPs such as NaCl,[34] homocysteine,[35] and poly lysine (a polymeric amine, M.W. 150, 000−300, 000)[36] were further employed to inspect the antiaggregation effect. The addition of NaCl, homocysteine, and poly lysine resulted in extensive aggregations of the Au NPs in the absence of HSA. After being incubated with 300 nM HSA for 15 min, the Au NPs exhibited excellent colloidal stability against these aggregating agents (Supporting Information, Figure S2), which suggests that the antiaggregation effect and may be a general strategy for design of optical sensing systems based on Au NPs.

A Colorimetric Method for HSA Detection and an INHIBIT Logic Gate Based on the Antiaggregation Effect. Intrigued by the fact that the antiaggregation effect is highly dependent on the concentration of HSA (Figure 2C), a colorimetric method is developed for quantitative detection of HSA. Figure 4, panel A showed the UV−vis spectra of the Au NPs (2.0 nM) mixed with different concentrations of HSA for 15 min, followed by the addition of melamine (20 μM). With the increased concentrations of HSA, intensity of the absorbance at 520 nm corresponding to the dispersed Au NPs increased gradually, and that at 650 nm corresponding to the aggregated ones decreased gradually. The values of A_{650}/A_{520} decreased with the increased concentrations of HSA, and the concentration calibration curve presented a linear relationship in the range of 20−100 nM (Figure 4B and insert), which indicates that the antiaggregation effect can be used to develop a colorimetric method for quantitative detection of HSA. Variations in concentrations of HSA also resulted in changes in color of the Au NPs from blue to purple, and then to red, which indicates the possibility of evaluation of the HSA concentration with the naked eye (Figure 4C).

Limit of detection (LOD) for the colorimetric method is estimated to be 1.4 nM based on IUPAC recommendations,[37] LOD = $3s_b/m$, in which s_b is the relative standard deviation of the blank sample obtained by analyzing ten samples containing the Au NPs (2.0 nM) and melamine (20 μM) in the absence of HSA, and m is the slope of the calibration curve. This LOD value can be further validated by the following experiment. In the absence and presence of 1.4 nM HSA, addition of 20 μM melamine resulted in distinguishable change in UV−vis spectral measurements (Supporting Information, Figure S3). This LOD value is much lower than the clinical threshold of HSA (~20 mg/L, ~ 300 nM) and is comparable to most of the current assays for HSA determination.[10−12] It should be noted that the linear detection range of the assay can be tuned readily by adjusting the concentration of melamine. For example, the detection range of HSA was shifted to 40−200 nM when the

DOI: 10.1021/acsami.5b01552
ACS Appl. Mater. Interfaces 2015, 7, 8990−8998

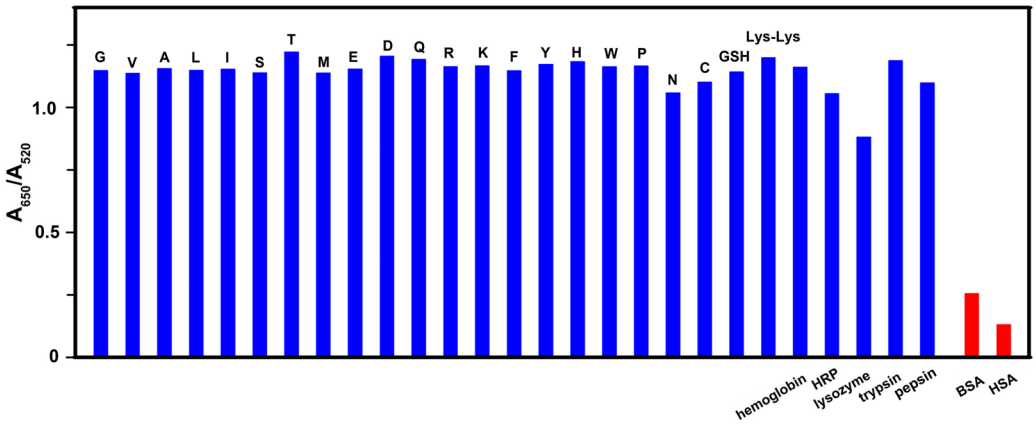

Figure 6. Values of the A_{650}/A_{520} ratios of the Au NPs incubated with 300 nM of amino acids, peptides, and proteins for 15 min, followed by the addition of melamine. The blue bars represent the aggregated state of the Au NPs, while the red bars represent the dispersed state of the Au NPs. The concentrations of the Au NPs and melamine were set at 2.0 nM and 20 μM, respectively.

concentration of melamine increased to 80 μM (Supporting Information, Figure S4).

The antiaggregation strategy can be extended to the design of a colorimetric binary INHIBIT logic gate. The INHIBIT logic is represented by the situation where the output is "1" only if one particular input is "1" and the other is "0". Additions of HSA and melamine are used as binary inputs, and color of the Au NPs is employed as the output to perform the INHIBIT gate. The absence and presence of each input are defined as "0" and "1", respectively. The blue color corresponding to the aggregated Au NPs (usually $A_{650}/A_{520} \geq 0.8$) is defined as output "1", and the red color corresponding to the dispersed Au NPs is defined as "0".[21] As shown in Figure 5, in the absence of both inputs or in the presence of HSA input alone, the Au NPs were well dispersed in the dispersion, corresponding to a red color (output = 0). The addition of melamine resulted in aggregation of the Au NPs, accompanied by change in color of the Au NPs from red to blue (output = 1). In the presence of both inputs, aggregation of the Au NPs induced by melamine was inhibited effectively due to the presence of HSA. Color of the Au NPs remained red (output = 0) at this time, which supports the INHIBIT logic function. The colorimetric response of the INHIBIT gate can be obtained in 1 min and be directly observed by the naked eye. Because of its low cost, rapid response, and ease of readout, the INHIBIT gate may be potentially useful in point-of-care applications in medical diagnosis.

Application of the Method for Detection of HSA in a Biological Sample. A biological sample was prepared to check the feasibility of the antiaggregation effect-based colorimetric method. Biological samples are known to be complex matrixes possibly containing various biomolecules. Thus, selectivity of the colorimetric method should be of particular concern. For example, amino acids and small peptides are often found in human urine and blood as metabolites. Previous studies demonstrated that amino acids and peptides are usually adsorbed on the surface of Au NPs through their amino groups and thiol groups (for cysteine and glutathione).[38−40] Here, the selectivity was evaluated by testing the response of the assay to a variety of amino acids and small peptides, including glycine (G), valine (V), alanine (A), leucine (L), isoleucine (I), serine (S), threonine (T), methionine (M), glutamic acid (E), aspartic acid (D), glutamine (Q), arginine (R), lysine (K), phenylalanine (F), tyrosine (Y), histidine (H), tryptophan (W), proline (P), asparagine (N), cysteine (C), glutathione (GSH), and lysine−lysine (Lys−Lys). In addition, biological samples usually contain a certain amount of other proteins besides HSA such as hemoglobin, horseradish peroxidase (HRP), lysozyme, trypsin, and pepsin, which may interact with Au NPs through their amino acid residues. Thus, selectivity of the colorimetric method toward these proteins was also investigated. As shown in Figure 6, when HSA was added first, addition of melamine resulted in a very low value of A_{650}/A_{520} (~0.1), which indicates that the aggregation of the Au NPs was effectively inhibited. However, much higher values of A_{650}/A_{520} (>0.8) were obtained when various other biomolecules (except BSA) were added into the Au NPs first, followed by the addition of melamine, which reveals that these biomolecules were not as effective as HSA to inhibit the aggregation of the Au NPs induced by melamine.

Such selectivity of the colorimetric method for HSA detection may be attributed to both the specific structure and the size of HSA. HSA contains a free cysteine residue (cysteine-34) exposed on the protein surface, which can covalently bind on Au NPs through the formation of Au−S bond. It has been reported that the cysteine residue is critical in maintaining the stability of Au NPs against aggregation.[39,40] Accordingly, the fact that amino acids, peptides, and proteins investigated here failed to protect the Au NPs against the melamine-induced aggregation is supposed to be due to the lack of free cysteine residues exposed on the surfaces (except cysteine and glutathione). In addition, although cysteine and glutathione bear free cysteine groups that allow their binding to the surface of Au NPs through the formation of Au−S bonds, they present almost no antiaggregation effect. These results suggest that the steric hindrance of HSA should also contribute to the selectivity, since the sizes of cysteine and glutathione are only ~0.6 nm and 1.5 × 0.4 nm^2, respectively,[41,42] while the size of HSA is about 8.4 × 3.2 nm^2. Indeed, it is noted that this method cannot distinguish HSA from BSA, which also contains a free cysteine residue exposed on the surface and has a size comparable with HSA. Considering that cysteine accounts for only 2% of amino acid residues in mammalian proteins, and most of the cysteine residues exist in the form of disulfide bond in the proteins,[39,43] this colorimetric method is still potentially useful in applications for biological analysis and clinical diagnosis.

DOI: 10.1021/acsami.5b01552
ACS Appl. Mater. Interfaces 2015, 7, 8990−8998

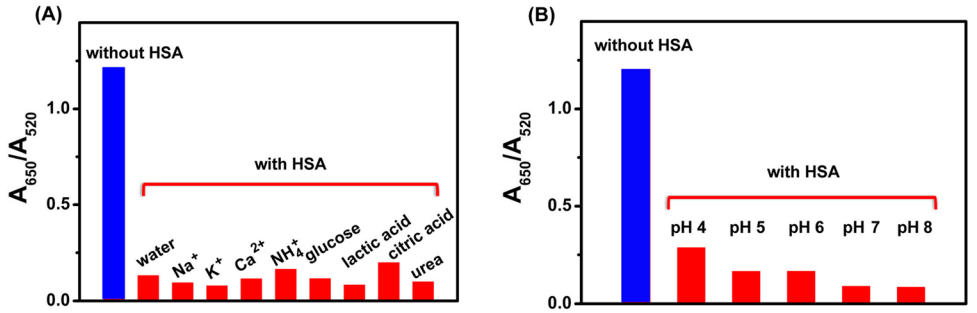

Figure 7. Values of the A_{650}/A_{520} ratios of the Au NPs incubated with HSA for 15 min (A) in the presence of Na^+ (25 mM), K^+ (25 mM), NH_4^+ (25 mM), Ca^{2+} (2.5 mM), glucose (20 mM), lactic acid (2 mM), citric acid (2 mM), or urea (1 M), respectively, and (B) under different pH values, followed by the addition of melamine. The blue bars represent the aggregated state of the Au NPs, while the red bars represent the dispersed state of the Au NPs. The concentrations of the Au NPs, HSA, and melamine were set at 2.0 nM, 300 nM, and 20 μM, respectively.

Table 1. Detection of HSA in Artificial Urine Samples by Using the Proposed Method and BCA Kit

		proposed method			BCA methods		
sample	spiked HSA (mg/L)	determined (mg/L)	recovery (%)	RSD (%, n = 3)	determined (mg/L)	recovery (%)	RSD (%, n = 3)
1	15	14.5	96.7	1.7	15.1	100.7	3.6
2	20	19.7	98.5	1.3	19.5	97.5	1.5
3	40	41.5	103.8	4.6	41.2	100.3	4.4

In fact, biological samples usually contain a large variety of ions and compounds, such as Na^+, K^+, NH_4^+, Ca^{2+}, glucose, lactic acid, citric acid, urea, etc., which may interfere in the reliability of the assay. Performance of the assay in the presence of these possible interfering substances was further evaluated. As shown in Figure 7, panel A, the Au NPs incubated with HSA were well dispersed in the presence of these possible interfering ions and compounds, followed by the addition of melamine. Urea is a well-known protein denaturant, and the minimum concentration of urea required to denature the protein is about 5 M.[44,45] In our experiments, addition of 1 M urea (maximum concentration of urea in human urine) had no significant effect on the structure of HSA and the antiaggregation effect (Supporting Information, Figure S5). It is known that in some disease states such as chronic renal failure and liver cirrhosis, partial denaturation of HSA will occur.[46−48] Thus, the feasibility of the antiaggregation effect on the partially denatured HSA was investigated. The partially denatured HSA was obtained by heating the protein to 75 °C for 15 min.[49−51] The CD spectra of native HSA exhibited two characteristic negative bands of α-helix at 208 and 218 nm[52,53] (Supporting Information, Figure S6A). The α-helicity of HSA, calculated by Payne's method, decreased from 41% to 31% after the heating process, which indicates the partial denaturing of the protein.[52,53] It was identified that the partially denatured HSA was also effective to protect the Au NPs against the melamine-induced aggregation (Supporting Information, Figure S6B). The pH value is another important parameter for biological samples, which is usually located in the range of 5−8. As shown in Figure 7, panel B, the HSA-covered Au NPs presented excellent stability in the range of pH 4−8 in the presence of 20 μM melamine.

On the basis of the above results, feasibility of the assay for HSA detection in artificial urine was tested. The calibration curve reveals that the value of A_{520}/A_{650} is in good linear relationship with the concentration of HSA in the range of 1.0−5.0 mg/L (1.0 mg/L = 15.0 nM) (Supporting Information, Figure S7), which indicates that the colorimetric method is qualified for quantitative detection of HSA in the artificial urine sample. For patients with diabetes and cardiovascular diseases, the concentration of HSA in their urine samples is usually higher than 20 mg/L, which is beyond the linear detection range of this method. Considering that the present method involves the mixing of the urine samples and the dispersion of the Au NPs, addition of suitable volume of the Au NPs dispersion can make the final concentration of HSA locate in the desired linear range without additional dilution. Typically, 50 μL of urine sample containing different concentrations of spiked HSA was added into 415 μL dispersion of the Au NPs (2.4 nM) and incubated for 15 min, then 25 μL of water and 10 μL of melamine (1.0 mM) were added (total volume of the sample was 500 μL, corresponding to a 10-fold dilution of the original samples). The concentrations of HSA in the samples were determined through the calibration curve. As shown in Table 1, the method shows good recoveries (96.0−103.0%) and reasonable relative standard deviations (<5.0%) for detection of HSA in the artificial urine samples. The results acquired by using this assay are in good agreement with those obtained by using the commercial BCA kit. According to the standard protocol of the BCA kit, it is required for the samples to be incubated with BCA reagent at 60 °C for 1 h; in comparison, the present assay can be carried out conveniently at room temperature no longer than 30 min.

CONCLUSION

In conclusion, a facile method was developed for quantitative detection of HSA by using Au NPs as the colorimetric probes. The method relies on the fact that HSA can protect the Au NPs against the melamine-induced aggregation. The possible mechanism for the antiaggregation effect is that the adsorption of HSA on the particle surface prevents the close approaching of neighboring Au NPs by steric hindrance or inhibits the effective cross-linking of neighboring Au NPs by melamine. Such a method addressing the concerns of low cost, easy operation, and excellent sensitivity as well as good selectivity, offers a promising platform for detection of HSA in biological samples. The antiaggregation effect can be further extended to fabricate an INHIBIT logic gate by using HSA and melamine as

DOI: 10.1021/acsami.5b01552
ACS Appl. Mater. Interfaces 2015, 7, 8990−8998

inputs and the color changes of Au NPs as outputs, which may have application potentials in point-of-care medical diagnosis.

■ ASSOCIATED CONTENT

Supporting Information

UV−vis absorption spectra of Au NPs in the absence and presence of 1.4 nM HSA followed by the addition of 20 μM melamine. Values of absorption ratio A_{650}/A_{520} of Au NPs incubated with different concentrations of HSA followed by the addition of 80 μM melamine. DLS measurements. The antiaggregation effect against other aggregating agents. The CD spectra of HSA in the absence and presence of urea. The CD spectra of native HSA and denatured HSA. Concentration calibration curve of the method in artificial urine. This material is available free of charge via the Internet at http://pubs.acs.org.

■ AUTHOR INFORMATION

Corresponding Author

*E-mail: wsyang@jlu.edu.cn.

Notes

The authors declare no competing financial interest.

■ ACKNOWLEDGMENTS

Financial support was provided by National Basic Research Program of China (No. 2011CB935800), the National Natural Science Foundation of China (No. 21303071, 51372097), and the China Postdoctoral Science Foundation (No. 2012M529670).

■ REFERENCES

(1) Westermeier, R.; Marouga, R. Protein Detection Methods in Proteomics Research. *Biosci. Rep.* **2005**, *25*, 19−32.

(2) Zhang, Y.; Guo, Y. M.; Xianyu, Y. L.; Chen, W. W.; Zhao, Y. Y.; Jiang, X. Y. Nanomaterials for Ultrasensitive Protein Detection. *Adv. Mater.* **2013**, *25*, 3802−3819.

(3) Doumas, B. T.; Peters, T., Jr. Serum and Urine Albumin: A Progress Report on Their Measurement and Clinical Significance. *Clin. Chim. Acta* **1997**, *258*, 3−20.

(4) Arques, S.; Ambrosi, P. Human Serum Albumin in the Clinical Syndrome of Heart Failure. *J. Card. Failure* **2011**, *17*, 451−458.

(5) Fanali, G.; di Masi, A.; Trezza, V.; Marino, M.; Fasano, M.; Ascenzi, P. Human Serum Albumin: From Bench to Bedside. *Mol. Aspects Med.* **2012**, *33*, 209−290.

(6) Tu, M. C.; Chang, Y. T.; Kang, Y. T.; Chang, H. Y.; Chang, P.; Yew, T. R. A Quantum Dot-Based Optical Immunosensor for Human Serum Albumin Detection. *Biosens. Bioelectron.* **2012**, *34*, 286−290.

(7) Caballero, D.; Martinez, E.; Bausells, J.; Errachid, A.; Samitier, J. Impedimetric Immunosensor for Human Serum Albumin Detection on a Direct Aldehyde-Functionalized Silicon Nitride Surface. *Anal. Chim. Acta* **2012**, *720*, 43−48.

(8) Contois, J. H.; Hartigan, C.; Rao, L. V.; Snyder, L. M.; Thompson, M. J. Analytical Validation of an HPLC Assay for Urinary Albumin. *Clin. Chim. Acta* **2006**, *367*, 150−155.

(9) Singh, R.; Crow, F. W.; Babic, N.; Lutz, W. H.; Lieske, J. C.; Larson, T. S.; Kumar, R. A Liquid Chromatography−Mass Spectrometry Method for the Quantification of Urinary Albumin Using a Novel ^{15}N-Isotopically Labeled Albumin Internal Standard. *Clin. Chem.* **2007**, *53*, 540−542.

(10) Chen, X. T.; Xiang, Y.; Tong, A. J. Facile, Sensitive, and Selective Fluorescence Turn-on Detection of HSA/BSA in Aqueous Solution Utilizing 2,4-Dihydroxyl-3-iodo Salicylaldehyde Azine. *Talanta* **2010**, *80*, 1952−1958.

(11) Wang, X. H.; Wang, X. Y.; Wang, Y. Q.; Guo, Z. J. Terbium(III) Complex as a Luminescent Sensor for Human Serum Albumin in Aqueous Solution. *Chem. Commun.* **2011**, *47*, 8127−8129.

(12) Sun, H. X.; Xiang, J. F.; Zhang, X. F.; Chen, H. B.; Yang, Q. F.; Li, Q.; Guan, A. J.; Shang, Q.; Tang, Y. L.; Xu, G. Z. A Colorimetric and Fluorometric Dual-Modal Supramolecular Chemosensor and Its Application for HSA Detection. *Analyst* **2014**, *139*, 581−584.

(13) Chai, F.; Wang, C. G.; Wang, T. T.; Li, L.; Su, Z. M. Colorimetric Detection of Pb^{2+} Using Glutathione Functionalized Gold Nanoparticles. *ACS Appl. Mater. Interfaces* **2010**, *2*, 1466−1470.

(14) Yanga, C.; Wang, Y.; Martyc, J. L.; Yang, X. R. Aptamer-Based Colorimetric Biosensing of Ochratoxin A Using Unmodified Gold Nanoparticles Indicator. *Biosens. Bioelectron.* **2011**, *26*, 2724−2727.

(15) Saha, K.; Agasti, S. S.; Kim, C.; Li, X.; Rotello, V. M. Gold Nanoparticles in Chemical and Biological Sensing. *Chem. Rev.* **2012**, *112*, 2739−2779.

(16) He, K.; Li, J.; Ni, Y. Y.; Fu, R.; Huang, Z. Z.; Yang, W. S. Effects of Cu^{2+} on Aggregation Behavior of Poly(L-Glutamic Acid)-Functionalized Gold Nanoparticles. *J. Nanopart. Res.* **2013**, 15.

(17) Si, S.; Kotal, A.; Mandal, T. K. One-Dimensional Assembly of Peptide-Functionalized Gold Nanoparticles: An Approach toward Mercury Ion Sensing. *J. Phys. Chem. C* **2007**, *111*, 1248−1255.

(18) Lin, M. H.; Pei, H.; Yang, F.; Fan, C. H.; Zuo, X. L. Applications of Gold Nanoparticles in the Detection and Identification of Infectious Diseases and Biothreats. *Adv. Mater.* **2013**, *25*, 3490−3496.

(19) Guo, L. Q.; Zhong, J. H.; Wu, J. M.; Fu, F. F.; Chen, G. N.; Zheng, X. Y.; Lin, S. Visual Detection of Melamine in Milk Products by Label-Free Gold Nanoparticles. *Talanta* **2010**, *82*, 1654−1658.

(20) Chi, H.; Liu, B. H.; Guan, G. J.; Zhang, Z. P.; Han, M. Y. A Simple, Reliable, and Sensitive Colorimetric Visualization of Melamine in Milk by Unmodified Gold Nanoparticles. *Analyst* **2010**, *135*, 1070−1075.

(21) Du, J. J.; Yin, S. Y.; Jiang, L.; Ma, B.; Chen, X. D. A Colorimetric Logic Gate Based on Free Gold Nanoparticles and the Coordination Strategy between Melamine and Mercury Ions. *Chem. Commun.* **2013**, *49*, 4196−4198.

(22) Jiang, Q.; Wang, Z. G.; Ding, B. Q. Programmed Colorimetric Logic Devices Based on DNA−Gold Nanoparticle Interactions. *Small* **2013**, *9*, 1016−1020.

(23) Deng, H. H.; Li, G. W.; Lin, X. H.; Liu, A. L.; Chen, W.; Xia, X. H. An IMPLICATION Logic Gate Based on Citrate-Capped Gold Nanoparticles with Thiocyanate and Iodide as Inputs. *Analyst* **2013**, *138*, 6677−6682.

(24) Huang, Z. Z.; Wang, H. N.; Yang, W. S. Glutathione-Facilitated Design and Fabrication of Gold Nanoparticle-Based Logic Gates and Keypad Lock. *Nanoscale* **2014**, *6*, 8300−8305.

(25) Ji, X. H.; Song, X. N.; Li, J.; Bai, Y. B.; Yang, W. S.; Peng, X. G. Size Control of Gold Nanocrystals in Citrate Reduction: The Third Role of Citrate. *J. Am. Chem. Soc.* **2007**, *129*, 13939−13948.

(26) Vangala, K.; Ameer, F.; Salomon, G.; Le, V.; Lewis, E.; Yu, L. Y.; Liu, D.; Zhang, D. M. Studying Protein and Gold Nanoparticle Interaction Using Organothiols as Molecular Probes. *J. Phys. Chem. C* **2012**, *116*, 3645−3652.

(27) Qu, Z. Y.; Chen, K. M.; Gu, H. C.; Xu, H. Covalent Immobilization of Proteins on 3D Poly(acrylic acid) Brushes: Mechanism Study and a More Effective and Controllable Process. *Bioconjugate Chem.* **2014**, *25*, 370−378.

(28) Zhou, Y.; Zhou, T. S.; Zhang, M.; Shi, G. Y. A DNA-Scaffolded Silver Nanocluster/Cu^{2+} Ensemble as a Turn-on Fluorescent Probe for Histidine. *Analyst* **2014**, *139*, 3122−3126.

(29) Liu, Y.; Deng, C. M.; Tang, L.; Qin, A. J.; Hu, R. R.; Sun, J. Z.; Tang, B. Z. Specific Detection of D-Glucose by a Tetraphenylethene-Based Fluorescent Sensor. *J. Am. Chem. Soc.* **2011**, *133*, 660−663.

(30) Wang, Y.; Ni, Y. N. Combination of UV−vis Spectroscopy and Chemometrics To Understand Protein−Nanomaterial Conjugate: A Case Study on Human Serum Albumin and Gold Nanoparticles. *Talanta* **2014**, *119*, 320−330.

(31) Dominguez-Medina, S.; McDonough, S.; Swanglap, P.; Landes, C. F.; Link, S. In Situ Measurement of Bovine Serum Albumin Interaction with Gold Nanospheres. *Langmuir* **2012**, *28*, 9131−9139.

(32) Templeton, A. C.; Pietron, J. J.; Murray, R. W.; Mulvaney, P. Solvent Refractive Index and Core Charge Influences on the Surface

DOI: 10.1021/acsami.5b01552
ACS Appl. Mater. Interfaces 2015, 7, 8990−8998

Plasmon Absorbance of Alkanethiolate Monolayer-Protected Gold Clusters. *J. Phys. Chem. B* **2000**, *104*, 564−570.
(33) Yan, H.; Wu, J. Y.; Dai, G. L.; Zhong, A. G.; Yang, J. G.; Liang, H. D.; Pan, F. Y. Interaction between Melamine and Bovine Serum Albumin: Spectroscopic Approach and Density Functional Theory. *J. Mol. Struct.* **2010**, *967*, 61−64.
(34) Dominguez-Medina, S.; Blankenburg, J.; Olson, J.; Landes, C. F.; Link, S. Adsorption of a Protein Monolayer via Hydrophobic Interactions Prevents Nanoparticle Aggregation under Harsh Environmental Conditions. *ACS Sustainable Chem. Eng.* **2013**, *1*, 833−842.
(35) Vangala, K.; Siriwardana, K.; Vasquez, E. S.; Xin, Y.; Pittman, C. U., Jr.; Walters, K. B.; Zhang, D. M. Simultaneous and Sequential Protein and Organothiol Interactions with Gold Nanoparticles. *J. Phys. Chem. C* **2013**, *117*, 1366−1374.
(36) Adhikari, M. D.; Panda, B. R.; Vudumula, U.; Chattopadhyay, A.; Ramesh, A. A Facile Method for Estimating Viable Bacterial Cells in Solution Based on "Subtractive-Aggregation" of Gold Nanoparticles. *RSC Adv.* **2012**, *2*, 1782−1793.
(37) Long, G. L.; Winefordner, J. D. Limit of Detection: A Closer Look at the IUPAC Definition. *Anal. Chem.* **1983**, *55*, 712−724.
(38) Ooka, A. A.; Kuhar, K. A.; Cho, N. J.; Garrella, R. L. Surface Interactions of a Homologous Series of α, ω-Amino Acids on Colloidal Silver and Gold. *Biospectroscopy* **1999**, *5*, 9−17.
(39) Siriwardana, K.; Wang, A. L.; Vangala, K.; Fitzkee, N.; Zhang, D. M. Probing the Effects of Cysteine Residues on Protein Adsorption onto Gold Nanoparticles Using Wild-Type and Mutated GB3 Proteins. *Langmuir* **2013**, *29*, 10990−10996.
(40) Kah, J. C. Y.; Chen, J.; Zubieta, A.; Hamad-Schifferli, K. Exploiting the Protein Corona around Gold Nanorods for Loading and Triggered Release. *ACS Nano* **2012**, *6*, 6730−6740.
(41) Liu, W. H.; Choi, H. S.; Zimmer, J. P.; Tanaka, E.; Frangioni, J. V.; Bawendi, M. Compact Cysteine-Coated CdSe(ZnCdS) Quantum Dots for in Vivo Applications. *J. Am. Chem. Soc.* **2007**, *129*, 14530−14531.
(42) Taladriz-Blanco, P.; Pastoriza-Santos, V.; Pérez-Juste, J.; Hervés, P. Controllable Nitric Oxide Release in the Presence of Gold Nanoparticles. *Langmuir* **2013**, *29*, 8061−8069.
(43) Requejo, R.; Hurd, T. R.; Costa, N. J.; Murphy, M. P. Cysteine Residues Exposed on Protein Surfaces Are the Dominant Intramitochondrial Thiol and May Protect against Oxidative Damage. *FEBS J.* **2010**, *277*, 1465−1480.
(44) Tanaka, N.; Nishizawa, H.; Kunugi, S. Structure of Pressure-Induced Denatured State of Human Serum Albumin: A Comparison with the Intermediate in Urea-Induced Denaturation. *Biochim. Biophys. Acta* **1997**, *1338*, 13−20.
(45) Miller, W. G.; Bruns, D. E.; Hortin, G. L.; Sandberg, S.; Aakre, K. M.; McQueen, M. J.; Itoh, Y.; Lieske, J. C.; Seccombe, D. W.; Jones, G. Current Issues in Measurement and Reporting of Urinary Albumin Excretion. *Clin. Chem.* **2009**, *55*, 24−38.
(46) Kozhevnikov, A. D. Modified Serum Albumin in the Pathogenesis of Glomerular Diseases: A New Hypothesis. *Arch. Int. Med.* **2002**, *162*, 356−358.
(47) Clavant, S. P.; Comper, W. D. Urinary Clearance of Albumin Is Critically Determined by Its Tertiary Structure. *J. Lab. Clin. Med.* **2003**, *142*, 372−384.
(48) Bito, R.; Hino, S.; Baba, A.; Tanaka, M.; Watabe, H.; Kawabata, H. Degradation of Oxidative Stress-Induced Denatured Albumin in Rat Liver Endothelial Cells. *Am. J. Physiol. Cell Physiol.* **2005**, *289*, 531−542.
(49) Sinha, S. S.; Mitra, R. K.; Pal, S. K. Temperature-Dependent Simultaneous Ligand Binding in Human Serum Albumin. *J. Phys. Chem. B* **2008**, *112*, 4884−4891.
(50) Rezaei-Tavirani1, M.; Moghaddamnia, S. H.; Ranjbar, B.; Amani, M.; Marashi, S. Conformational Study of Human Serum Albumin in Predenaturation Temperatures by Differential Scanning Calorimetry, Circular Dichroism, and UV Spectroscopy. *J. Biochem. Mol. Biol.* **2006**, *39*, 530−536.
(51) Holm, N. K.; Jespersen, S. K.; Thomassen, L. V.; Wolff, T. Y.; Sehgal, P.; Thomsen, L. N.; Christiansen, G.; Andersen, C. B.; Knudsen, A. D.; Otzen, D. E. Aggregation and Fibrillation of Bovine Serum Albumin. *Biochim. Biophys. Acta* **2007**, *1774*, 1128−1138.
(52) Fleischer, C. C.; Payne, C. K. Secondary Structure of Corona Proteins Determines the Cell Surface Receptors Used by Nanoparticles. *J. Phys. Chem. B* **2014**, *118*, 14017−14026.
(53) Fleischer, C. C.; Payne, C. K. Nanoparticle−Cell Interactions: Molecular Structure of the Protein Corona and Cellular Outcomes. *Acc. Chem. Res.* **2014**, *47*, 2651−2659.

DOI: 10.1021/acsami.5b01552
ACS Appl. Mater. Interfaces 2015, 7, 8990−8998